A MULTISCALE FORMULATION OF THE DISCONTINUOUS PETROV-GALERKIN METHOD FOR ADVECTIVE-DIFFUSIVE PROBLEMS

CARLO L. BOTTASSO[†], STEFANO MICHELETTI[‡], AND RICCARDO SACCO[‡]

Abstract. We consider the Discontinuous Petrov-Galerkin method for the advection-diffusion model problem, and we investigate the application of the variational multiscale method to this formulation. We show the exact modeling of the fine scale modes at the element level for the linear case, and we discuss the approximate modeling both in the linear and in the non-linear cases. Furthermore, we highlight the existing link between this multiscale formulation and the p version of the finite element method. Numerical examples illustrate the behavior of the proposed scheme.

Key words. Finite element method, mixed and hybrid methods, discontinuous Galerkin, Petrov-Galerkin, advection-diffusion problem, variational multiscale method

AMS subject classifications. 65N30

1. Introduction and Motivation. We have recently introduced the Discontinuous Petrov-Galerkin (DPG) method for the solution of elliptic problems [5] and isotropic/anisotropic linear compressible and incompressible elasticity (Stokes problem) [3, 8]. We propose in these pages some remarks on the application of the DPG method to the advection-diffusion model problem in one spatial dimension. This is a necessary step towards the extension of the method to the compressible and incompressible Navier-Stokes equations, our final goal.

As shown in ref. [1], most Discontinuous Galerkin (DG) methods can be classified according to the selection of a specific expression for the "numerical fluxes" that are used for connecting neighboring elements. This expression, together with the choice of the functional spaces, effectively characterizes each method. The numerical fluxes are defined by expressing the element interface fields (e.g., edge variables in two spatial dimensions, or face variables in three spatial dimensions) as suitable averages of the internal fields for the elements sharing that interface. Slightly deviating from this philosophy, in the DPG method *all unknown fields are approximated by internal and boundary variables*, as it is usually done in mixed-hybrid formulations. The internal (mixed) variables are discontinuous across element interfaces as in other DG methods. However the boundary (hybrid) variables, while maintaining their classical role of connectors, are in this case treated as additional problem unknowns. Therefore, we do not have to select a recipe up-front in order to explicitly define the connectors in terms of the internal variables for formulating the method. This comes with a price to be paid, since it implies that the test and trial functions must now be chosen in different spaces, i.e. the resulting method is a mixed-hybrid Petrov-Galerkin one. It can be rigorously shown that this process yields higher order accurate interface unknowns (see [2, 5] and [7] for the analysis in one and two spatial dimensions, respectively). This behavior has also been experimentally observed in higher dimensional problems (see [5, 7]).

It is well known that most numerical schemes fail to properly treat the finer

[†]D. Guggenheim School of Aerospace Engineering, Georgia Institute of Technology, 270 Ferst Dr., 30332-0150 Atlanta GA, USA (carlo.bottasso@ae.gatech.edu).

[‡]MOX–Modeling and Scientific Computing, Dipartimento di Matematica "F. Brioschi", Politecnico di Milano, Via Bonardi 9, 20133 Milano, Italy (stefano.micheletti@mate.polimi.it, riccardo.sacco@mate.polimi.it).

solution scales, that consequently appear as abnormally amplified in the computed solution. The variational multiscale method [11] is a recent attempt at incorporating these effects in a finite element based numerical process, with the additional result of unifying some very successful previous methods, in particular those based on the stabilized and the residual-free bubble concepts [6]. We shall apply the variational multiscale framework to the DPG method in the following pages. This presents some interest since we are dealing with a mixed-hybrid method in Petrov-Galerkin form. The application of the multiscale framework to a mixed-hybrid formulation is a point that, to our knowledge, has been touched only very briefly in the literature. Our treatment here of this material is far from exhaustive but it is practically oriented and gives some interesting results. In particular, we develop general orthogonality conditions for the visible and invisible scales. These conditions allow hierarchical p approximations to be generated, while ensuring that each new enriching space is orthogonal to the ones already used for the modeling, i.e. it is not even partially already contained in them. Furthermore, we obtain a natural decoupling of the fine scale problems at the element level.

In this work, we address the advection-diffusion model problem in one spatial dimension with both linear and non-linear advective fluxes. More precisely, the paper is organized in the following manner. In section 2 we discuss the DPG method for the non-linear advection-diffusion model problem. Then we extend in section 3 the DPG formulation by incorporating into it the ideas of the variational multiscale method. In particular, we consider in section 3.1 the decomposition of both trial and test function spaces into coarse and fine scales, while in section 3.2 we discuss the solution of the coarse and fine scale subproblems arising from the application of the multiscale DPG formulation to a linearized advection-diffusion model problem. We apply the proposed discretization framework in section 4 to the linear advective-diffusive model problem. The exact treatment of subgrid scales is analyzed in section 4.1, while in section 4.2 we address the approximate treatment of subgrid scales. This allows us to establish the equivalence between a particular multiscale DPG method and a p-hierarchical finite element method. More remarks on this relationship are drawn in section 4.3. In section 4.4 we first briefly discuss the implementation of the multiscale DPG formulation as a standard nodal displacement finite element scheme, by applying the static condensation procedure of the internal variables in favor of the sole interface (displacement) variables. Next, we analyze, both theoretically and numerically in section 4.5, the stabilization effects of the multiscale DPG approach in the case of the lowest order member of the family of methods. To conclude the paper, we apply in section 5 the proposed method to a non-linear advective-diffusive model problem, namely the non-linear steady Burgers equation.

2. The Discontinuous Petrov-Galerkin Method. We consider the classical advection-diffusion model problem in conservative form and in one spatial dimension

$$-F_{\text{diff}}(u)_{,x} + F_{\text{adv}}(u)_{,x} = f \quad \text{in } \Omega \subset \mathbb{R}, \tag{2.1}$$

with boundary conditions

$$u = g \quad \text{on } \Gamma,$$

where $\Omega = (0, X)$, $\Gamma = \{0, X\}$ and f, g are given data. $F_{\text{adv}}(\cdot)$ is the advective flux, which is in general a non-linear function of the variable u, while

$$F_{\text{diff}}(\cdot) = \kappa \frac{d(\cdot)}{dx}$$

is the diffusive flux, κ being the diffusion coefficient which may depend on the space variable x but not on the variable u. For any function $v = v(x)$ we denote by $v_{,x}$ the spatial derivative of v with respect to x. The notation adopted above resembles the usual conservative form of the Navier-Stokes equations for compressible and incompressible fluids.

In view of the approximation of problem (2.1), we let $\{\mathcal{T}_h\}_{h>0}$ be a family of grids of $\overline{\Omega}$, K denoting a generic element. More precisely, we consider a partition $0 \equiv x_0 < x_1 < \ldots < x_{n-1} < x_n \equiv X$ composed of $n \geq 1$ intervals $K^i = [x_i, x_{i+1}]$ of size h^i, $i = 0, \ldots, n-1$, with $h = \max_i h^i$, and we indicate with $\mathcal{E}_h = \{x_i\}_{i=0}^n$ the set of nodes. Introducing the auxiliary unknown

$$\sigma = F_{\text{diff}}(u) = \kappa\, u_{,x}, \tag{2.2}$$

problem (2.1) can be reformulated in weak form over each element K of $\mathcal{T}_h$ as

$$\begin{cases} \displaystyle\int_K (-\sigma_{,x} + F_{\text{adv}}(u)_{,x}) v \, dx & \\ \displaystyle +((F_{\text{adv}}(\lambda) - F_{\text{adv}}(u)) - (\mu - \sigma))v|_{\partial K} = \int_K f v \, dx & \forall v \in V(K), \\ \displaystyle\int_K (\kappa^{-1}\sigma - u_{,x}) w \, dx - (\lambda - u) w|_{\partial K} = 0 & \forall w \in W(K), \end{cases} \tag{2.3}$$

where $V(K)$ and $W(K)$ are infinite dimensional spaces of sufficiently smooth functions defined on K, such that all the integrals in (2.3) are well defined. In this formulation, each element is characterized by *internal* fields u and σ, and by *interface* fields λ and μ that represent the traces of u and σ on ∂K, respectively. Consequently, equations (2.3) present integral terms that enforce in a weak sense the flux (2.1) and constitutive (2.2) equations over each element, in addition to boundary terms that enforce in a weak sense the continuity of the internal and interface fields.

After integration by parts, the weak form of problem (2.1) becomes:

find $u \in U$, $\sigma \in \Sigma$, $\lambda \in \Lambda_g$ and $\mu \in \Lambda$ such that $\forall K \in \mathcal{T}_h$ we have

$$\begin{cases} \displaystyle\int_K (\sigma - F_{\text{adv}}(u)) v_{,x} \, dx - (\mu - F_{\text{adv}}(\lambda)) v|_{\partial K} = \int_K f v \, dx & \forall v \in V(K), \\ \displaystyle\int_K \kappa^{-1}\sigma w \, dx + \int_K u w_{,x} \, dx - \lambda w|_{\partial K} = 0 & \forall w \in W(K), \end{cases} \tag{2.4}$$

where $U = \Sigma = L^2(\Omega)$, Λ is the space of functions defined only at the nodes of $\mathcal{T}_h$, Λ_g is the manifold of Λ made of functions equal to g at x_0 and x_n, and $V(K) = W(K) = H^1(K) = \left\{v \in L^2(K) \,|\, v_{,x} \in L^2(K) \forall K \in \mathcal{T}_h\right\}$.

The DPG discretization of the one-element weak formulation (2.4) reads:

find $u_h \in U_h$, $\sigma_h \in \Sigma_h$, $\lambda_h \in \Lambda_{g,h}$ and $\mu_h \in \Lambda_h$ such that $\forall K \in \mathcal{T}_h$ we have

$$\begin{cases} \displaystyle\int_K (\sigma_h - F_{\text{adv}}(u_h)) v_{h,x} \, dx - (\mu_h - F_{\text{adv}}(\lambda_h)) v_h|_{\partial K} = \int_K f v_h \, dx & \forall v_h \in V_h(K), \\ \displaystyle\int_K \kappa^{-1}\sigma_h w_h \, dx + \int_K u_h w_{h,x} \, dx - \lambda_h w_h|_{\partial K} = 0 & \forall w_h \in W_h(K). \end{cases} \tag{2.5}$$

REMARK 1. *Throughout the paper we refer to formulation (2.5) as the* plain DPG *method.* The local finite element space is

$$\mathbb{DPG}_h^k(K) = \{(u_h, \sigma_h, \lambda_h, \mu_h; v_h, w_h) \mid (u_h, \sigma_h, \lambda_h, \mu_h; v_h, w_h) \in \mathcal{U}_h(K) \times \mathcal{V}_h(K) \, \forall K \in \mathcal{T}_h\},$$

where we have set

$$\begin{aligned} \mathcal{U}_h(K) &= U_h(K) \times \Sigma_h(K) \times \Lambda_{g,h}(\partial K) \times \Lambda_h(\partial K), \\ \mathcal{V}_h(K) &= V_h(K) \times W_h(K). \end{aligned} \tag{2.6}$$

The local spaces are selected as

$$U_h(K) = \Sigma_h(K) = \mathbb{P}_k(K) \quad \text{and} \quad V_h(K) = W_h(K) = \mathbb{P}_{k+1}(K), \quad k \geq 0,$$

where $\mathbb{P}_k$ is the space of polynomials of degree equal to or less than k, while

$$\begin{aligned} \Lambda_h(\partial K) &= \left\{ \{\eta_k\}_{k=1}^2 \mid \eta_k \in \mathbb{R}, \text{ at the nodes of } K \right\} \\ \Lambda_{g,h}(\partial K) &= \left\{ \eta_h \in \Lambda_h(\partial K) \mid \eta_h = g \text{ if } \partial K \cap \Gamma \neq \emptyset \right\}. \end{aligned}$$

The global finite element space for the internal field u_h is

$$U_h = \left\{ u_h \in L^2(\Omega) \mid u_h|_K \in U_h(K) \, \forall K \in \mathcal{T}_h \right\}.$$

Analogously for the internal field σ_h, i.e. $\Sigma_h = U_h$. The global finite element space for the test functions v_h is

$$V_h = \left\{ v_h \in L^2(\Omega) \mid v_h|_K \in V_h(K) \, \forall K \in \mathcal{T}_h \right\},$$

and here again the same space is used for the test functions w_h, $W_h = V_h$. The global spaces for the interface unknowns are

$$\Lambda_h = \left\{ \{\eta_i\}_{i=0}^n \mid \eta_i \in \mathbb{R}, \, i = 0, \ldots, n \right\},$$

where functions are defined only at the nodes, and similarly

$$\Lambda_{g,h} = \left\{ \eta_h \in \Lambda_h \mid \eta_h = g \text{ if } i = 0 \text{ or } i = n \right\}.$$

Finally, the global finite element space is

$$\mathbb{DPG}_h^k = (U_h \times \Sigma_h \times \Lambda_{g,h} \times \Lambda_h) \times (V_h \times W_h).$$

Formulation (2.5) is of Petrov-Galerkin type, since different trial and test finite element spaces are used. It is also characterized by a completely symmetric treatment of both equations and both unknown fields. In fact, the flux and constitutive equations are integrated by parts; this has the consequence that both u_h and σ_h have the same identical continuity requirements. Hence, equal-order interpolation can be used for these variables.

Furthermore, it is important to realize that $u_h|_{\partial K} \neq \lambda_h$ and $\sigma_h|_{\partial K} \neq \mu_h$. In other words, there can be jump discontinuities at the element boundaries between the internal and the interface fields. These latter variables act as inter-element connectors, gluing together neighboring elements, and enjoy a higher convergence rate than the internal variables, as shown in refs. [5, 7] in the case of the elliptic model problem.

Since the internal variables are discontinuous across elements, they can be statically condensed leading to a linear system in the sole interface variables, as commonly done in mixed-hybrid formulations. Alternatively, one can render the test functions continuous at the nodes; this has the effect of eliminating the interface fields, and yields a discrete problem in the sole internal variables, which fits the method into the standard framework of DG formulations. The boundary unknowns can then be recovered through an element-by-element post-processing of the internal solution. Therefore, this scheme comes equipped with a consistent (no choice to perform a priori) and built-in way to recover higher order accurate boundary fluxes, i.e. there is no need to develop special post-processing techniques to recover this information as it might be necessary with other continuous (see ref. [10]) or discontinuous (see ref. [1]) formulations. An example of the static condensation procedure will be given in section 4.4, while more details about the application of this technique to the DPG formulation and the relationship between the DPG method and DG methods can be found in ref. [7].

In the next sections we show how to devise a stable discretization scheme for the advection-diffusion problem (2.1), by properly applying the variational multiscale philosophy proposed in [11] to the DPG formulation (2.5) introduced in the present article.

3. Multiscale Modeling and the DPG Method. The aim of the section is to prepare a proper discrete functional setting for a stable numerical approximation of the advection-diffusion problem (2.1) based on the DPG formulation (2.5), which, in the presence of strong advection is affected by numerical instabilities. In doing this, we modify the finite element structure of the method by considering the effects of *subgrid scales* on the computed solution. This strategy extends to the DPG formulation the idea of *variational multiscale modeling* recently proposed by Hughes and coworkers in ref. [11] and further analyzed by Brezzi in ref. [6]. As it will be shown in sections 4 and 5, the DPG formulation with multiscale modeling leads, at least in the case of the lowest order member of the DPG family, to a robust finite element discretization of the advection-diffusion equation (2.1) that maintains stability and accuracy even when the problem is strongly advection-dominated.

3.1. Coarse and Fine Scale Decomposition. The basic idea of the multiscale formulation is to consider an *augmented space* where problem (2.5) is to be solved for. The aim of the strategy is to enlarge, for a given mesh parameter h, the resolution of the original finite element space by decomposing the solution of the augmented problem into coarse (visible) and fine (invisible) scales. Eventually, the fine scales are eliminated in favor of the coarse ones (when the governing equations are linear) through a process that can be conveniently recognized (and implemented) as the classical procedure of *static condensation* (see [6] for a wider description of this subject).

We introduce therefore the augmented trial space

$$\mathcal{U}^A(K) = \mathcal{U}_h(K) + \mathcal{B}_{\mathcal{U}}(K), \tag{3.1}$$

where the space $\mathcal{U}_h(K)$ is defined in (2.6) and $\mathcal{B}_{\mathcal{U}}(K)$ is a trial bubble function space formally structured as

$$\mathcal{B}_{\mathcal{U}}(K) = B_u(K) \times B_\sigma(K) \times \{0\} \times \{0\} \qquad \forall K \in \mathcal{T}_h. \tag{3.2}$$

$B_u(K)$ and $B_\sigma(K)$ are yet unspecified *infinite dimensional* function spaces that represent the fine scales *augmenting* the finite element trial space of the DPG formulation.

As a consequence, we have the following spatially overlapping sum decomposition of the fields u_h and σ_h within each element K

$$u_h^A = \overline{u}_h + \widetilde{u}_h, \qquad \sigma_h^A = \overline{\sigma}_h + \widetilde{\sigma}_h \qquad \forall K \in \mathcal{T}_h, \tag{3.3}$$

with $\overline{u}_h \in U_h(K)$, $\overline{\sigma}_h \in \Sigma_h(K)$, $\widetilde{u}_h \in B_u(K)$, $\widetilde{\sigma}_h \in B_\sigma(K)$, and where $(\cdot)^A$ indicates now the *augmented* fields. Notice that *no* augmenting spaces are introduced for the interface variables. We shall come back to this point later on.

As a general rule (see [6]), the spaces $B_u(K)$ and $B_\sigma(K)$ should be chosen in such a way that (3.3) is a direct sum. Assuming that

$$\mathcal{U}^A(K) = L^2(K) \times L^2(K) \times \mathbb{R}^2 \times \mathbb{R}^2, \tag{3.4}$$

the most natural choice for selecting the bubble space is

$$B_u(K) = B_\sigma(K) = L^2(K) \setminus \mathbb{R} \qquad \forall K \in \mathcal{T}_h, \tag{3.5}$$

since the constant scale is already contained in the coarse trial space.

Two remarks are in order with the trial space decomposition (3.3). First, note that there is no boundary condition associated with the fine internal fields, since in the DPG method the role of supporting these conditions together with the continuity across elements is left to the interface fields. Therefore, we do not have to assume null fine scale modes on ∂K as in other finite element methods. The second remark is that in a one-dimensional problem, as the one considered here, there is no need to consider a splitting similar to (3.3) for the interface variables λ_h and μ_h. In fact, the fine scale modes could only amount to Dirac delta functions defined at the element nodes, which are however already contained in Λ_h and $\Lambda_{g,h}$. Therefore, the original and augmented spaces must coincide, and we can set in the following

$$\lambda_h^A = \overline{\lambda}_h, \qquad \mu_h^A = \overline{\mu}_h.$$

The situation would be different in multiple spatial dimensions, where one could have functions with local support on the edges or faces in order to model fine boundary scales.

Since the discrete formulation considered in this article is of a Petrov-Galerkin type, we have now to consider a sum decomposition of the test function space too. In analogy with (3.1), we set

$$\mathcal{V}^A(K) = \mathcal{V}_h(K) + \mathcal{B}_\mathcal{V}(K), \tag{3.6}$$

where $\mathcal{V}_h(K)$ is defined in (2.6) and $\mathcal{B}_\mathcal{V}(K)$ is a test bubble function space formally structured as

$$\mathcal{B}_\mathcal{V}(K) = B_v(K) \times B_w(K) \qquad \forall K \in \mathcal{T}_h. \tag{3.7}$$

Here again, $B_v(K)$ and $B_w(K)$ are yet unspecified *infinite dimensional* function spaces that represent the fine scales *augmenting* the finite element test space of the DPG formulation. As a consequence, we have the following spatially overlapping sum decomposition for the test functions

$$v_h^A = \overline{v}_h + \widetilde{v}_h, \qquad w_h^A = \overline{w}_h + \widetilde{w}_h, \qquad \forall K \in \mathcal{T}_h, \tag{3.8}$$

where $\overline{v}_h \in V_h(K)$, $\overline{w}_h \in W_h(K)$, $\widetilde{v}_h \in B_v(K)$ and $\widetilde{w}_h \in B_w(K)$. Assuming that

$$\mathcal{V}^A(K) = H^1(K) \times H^1(K), \tag{3.9}$$

the most natural choice for selecting the bubble space is

$$B_v(K) = B_w(K) = H^1(K) \setminus \mathbb{R} \qquad \forall K \in \mathcal{T}_h, \tag{3.10}$$

since, as before, the constant scale is already contained in the coarse test space.

Examples of the use of the multiscale decompositions (3.3) and (3.8) in the DPG formulation (2.5) will be shown in sections 4.1 and 4.2.

3.2. Coarse and Fine Scale Subproblems. Let us now employ the coarse and fine scale decompositions introduced in the previous section to construct a finite element approximation of (2.1) using the DPG formulation. With this aim, we insert (3.3) and (3.8) into (2.5), where the replacement $\mathcal{U}_h(K) \leftarrow \mathcal{U}^A(K)$ and $\mathcal{V}_h(K) \leftarrow \mathcal{V}^A(K)$ is understood, obtaining as a result a *non-linear* augmented problem. This latter problem is characterized by having unknowns of both *finite* ($\overline{u}_h$ and $\overline{\sigma}_h$) and *infinite* ($\widetilde{u}_h$ and $\widetilde{\sigma}_h$) dimensional nature.

REMARK 2. *Throughout the paper we refer to this augmented formulation as the* multiscale DPG *method.*

Unless otherwise stated, we assume henceforth that the problem at hand is linear, i.e. $F_{\text{adv}}(u) = au$, where in general $a = a(x)$ is the given advective speed. This allows us to simplify the exposition without giving up generality, since the non-linear case can be dealt with through linearization, e.g. via Newton's method, which yields a sequence of problems of the type (2.5) (see also section 5).

Following a standard procedure in multiscale variational formulations, it is convenient, though not necessary (as pointed out later on), to split the *linear augmented* problem into two coupled linear subproblems. The first subproblem (corresponding to taking $v_h = \overline{v}_h$ and $w_h = \overline{w}_h$ in (2.5)) determines the coarse scales accounting for the effects of the fine ones, and reads:

find $\overline{u}_h \in U_h(K)$, $\widetilde{u}_h \in B_u(K)$, $\overline{\sigma}_h \in \Sigma_h(K)$, $\widetilde{\sigma}_h \in B_\sigma(K)$, $\lambda_h \in \Lambda_{g,h}$ and $\mu_h \in \Lambda_h$ such that $\forall K \in \mathcal{T}_h$ we have

$$\begin{cases} \displaystyle\int_K (\overline{\sigma}_h - a\overline{u}_h)\overline{v}_{h,x}\,dx - (\overline{\mu}_h - a\overline{\lambda}_h)\overline{v}_h|_{\partial K} \\ \qquad \displaystyle + \int_K (\widetilde{\sigma}_h - a\widetilde{u}_h)\overline{v}_{h,x}\,dx = \int_K f\overline{v}_h\,dx \qquad \forall \overline{v}_h \in V_h(K), \\ \displaystyle\int_K \kappa^{-1}\overline{\sigma}_h\overline{w}_h\,dx + \int_K \overline{u}_h\overline{w}_{h,x}\,dx - \overline{\lambda}_h\overline{w}_h|_{\partial K} \\ \qquad \displaystyle + \int_K k^{-1}\widetilde{\sigma}_h\overline{w}_h\,dx + \int_K \widetilde{u}_h\overline{w}_{h,x}\,dx = 0 \qquad \forall \overline{w}_h \in W_h(K). \end{cases} \tag{3.11}$$

The second subproblem (corresponding to taking $v_h = \widetilde{v}_h$ and $w_h = \widetilde{w}_h$ in (2.5)) gives rise to a set of equations for the fine scales that are driven by the residuals of the coarse scales, and reads:

find $\overline{u}_h \in U_h(K)$, $\widetilde{u}_h \in B_u(K)$, $\overline{\sigma}_h \in \Sigma_h(K)$, $\widetilde{\sigma}_h \in B_\sigma(K)$, $\lambda_h \in \Lambda_{g,h}$ and $\mu_h \in \Lambda_h$

such that $\forall K \in \mathcal{T}_h$ we have

$$
\left\{
\begin{array}{ll}
\displaystyle\int_K (\widetilde{\sigma}_h - a\widetilde{u}_h)\widetilde{v}_{h,x}\,dx = \int_K r_h \widetilde{v}_h\,dx & \\
\qquad - \left((\overline{\sigma}_h - a\overline{u}_h) - (\overline{\mu}_h - a\overline{\lambda}_h)\right)\widetilde{v}_h|_{\partial K} & \forall \widetilde{v}_h \in B_v(K), \\
\displaystyle\int_K \kappa^{-1}\widetilde{\sigma}_h\widetilde{w}_h\,dx + \int_K \widetilde{u}_h\widetilde{w}_{h,x}\,dx = \int_K s_h\widetilde{w}_h\,dx & \\
\qquad -(\overline{u}_h - \overline{\lambda}_h)\widetilde{w}_h|_{\partial K} & \forall \widetilde{w}_h \in B_w(K),
\end{array}
\right. \tag{3.12}
$$

where we have set

$$
r_h = f + \overline{\sigma}_{h,x} - (a\overline{u}_h)_{,x}, \qquad s_h = -(\kappa^{-1}\overline{\sigma}_h - \overline{u}_{h,x}).
$$

Clearly, being able to solve the fine scale subproblem (3.12), one could eliminate the fine scale modes $\widetilde{u}_h$ and $\widetilde{\sigma}_h$ by back-substitution into the coarse scale subproblem (3.11), ending up with a linear system in the sole (finite dimensional) coarse scale unknowns $\overline{u}_h$ and $\overline{\sigma}_h$.

Some remarks are in order about the solution of the coarse and fine scale subproblems (3.11) and (3.12). First, we note that problem (3.12) states that the fine scale modes $\widetilde{u}_h$ and $\widetilde{\sigma}_h$ are driven by the residuals in the element interiors (r_h and s_h) and by the residuals at the element boundaries, i.e. the jump terms between internal and interface variables. As the mesh size h goes to zero, all residuals will tend to zero, and the fine scales will eventually disappear, as expected. In fact, when the mesh size is zero all scales are coarse, i.e. visible. The second remark is that, solving for the fine scale modes $\widetilde{u}_h$ and $\widetilde{\sigma}_h$ shows that the present formulation comes equipped with an automatic error estimator. In fact, assuming that a decomposition of the exact solution u, σ in terms of coarse and fine scales can be performed analogously to (3.3), we may define the *unresolved part* of the exact solution as

$$
u_{\text{unr}} = u - \overline{u} = \widetilde{u}, \qquad \sigma_{\text{unr}} = \sigma - \overline{\sigma} = \widetilde{\sigma}.
$$

According to the relative weight of coarse and fine scales, the quantities u_{unr} and σ_{unr} provide important information on the *local* behavior of the exact solution u, σ. Since in practice $\widetilde{u}$ and $\widetilde{\sigma}$ are clearly unknown, it is convenient to replace them with their approximations $\widetilde{u}_h$ and $\widetilde{\sigma}_h$, obtaining the following *computable relations*

$$
u_{\text{unr}} = \widetilde{u} \simeq \widetilde{u}_h, \qquad \sigma_{\text{unr}} = \widetilde{\sigma} \simeq \widetilde{\sigma}_h.
$$

These relations provide a simple (and hopefully effective) indicator to drive the grid adaptation process.

Having set up the variational multiscale framework for the DPG discretization of the (linearized) advective-diffusive model problem (2.1), we discuss in section 4 the implementation of the multiscale procedure and then conclude the presentation by applying the methodology in section 5 to the non-linear advective-diffusive model problem.

4. The Linear Advection-Diffusion Problem. An important observation that should be made concerning the multiscale DPG discretization of the one-dimensional linear advective-diffusive problem is that, since we do not have fine interface scales, problem (3.12) can be solved *independently on each individual element.* In fact, there is a natural decoupling of the fine scale problems, while the coupling

among elements is confined at the coarse level. This of course would not be true in a multi-dimensional problem. In this case, one might think of lowering the cost of the multiscale method by introducing some *localization* hypothesis in order to perform the computation of the fine scales on an element by element (or maybe patch of elements by patch of elements) basis. This would clearly come at the cost of some degraded performance, since the effects of the fine interface fields would be neglected in this case.

Integrating (3.12) on each element $K \in \mathcal{T}_h$ to obtain $\widetilde{u}_h$ and $\widetilde{\sigma}_h$ as functions of $\overline{u}_h$, $\overline{\sigma}_h$, $\overline{\lambda}_h$ and $\overline{\mu}_h$, and plugging the solution back into (3.11), one can then solve this latter problem in terms of $\overline{u}_h$, $\overline{\sigma}_h$, $\overline{\lambda}_h$ and $\overline{\mu}_h$. This can be done exactly for the present model problem. In general, for more complex operators or in multiple spatial dimensions, the exact elimination can not be performed, and it is then natural to seek a solution to the local (elemental) fine scale problem using an approximate method.

We analyze both the exact and the approximate modeling of fine scales in the following for the problem at hand. For simplicity, we limit the attention to the lowest order finite element space in the DPG family, denoted by $\mathbb{DPG}_h^0$. In this case, the trial functions for the internal coarse scales are constant within each element, and are written $\overline{u}_h|_{K^i} = \overline{u}^i$ and $\overline{\sigma}_h|_{K^i} = \overline{\sigma}^i$ for the i-th element. The elemental residuals are then simply

$$r_h = f - a_{,x}\overline{u}^i, \qquad s_h = -\kappa^{-1}\overline{\sigma}^i.$$

4.1. Exact Subgrid Model. Let us integrate by parts both terms at the left-hand side in (3.12) to obtain

$$\left\{\begin{array}{l} -\displaystyle\int_K (\widetilde{\sigma}_h - a\widetilde{u}_h)_{,x}\widetilde{v}_h\,dx + (\widetilde{\sigma}_h - a\widetilde{u}_h)\widetilde{v}_h|_{\partial K} = \int_K r_h\widetilde{v}_h\,dx \\ \qquad -\left((\overline{\sigma}_h - \overline{\mu}_h) - (a(\overline{u}_h - \overline{\lambda}_h)\right)\widetilde{v}_h|_{\partial K} \qquad \forall \widetilde{v}_h \in B_v(K), \\ \displaystyle\int_K (\kappa)^{-1}\widetilde{\sigma}_h\widetilde{w}_h\,dx - \int_K \widetilde{u}_{h,x}\widetilde{w}_h\,dx + (\widetilde{u}_h\widetilde{w}_h)|_{\partial K} = \int_K s_h\widetilde{w}_h\,dx \\ \qquad +(\overline{\lambda}_h - \overline{u}_h)\widetilde{w}_h|_{\partial K} \qquad \forall \widetilde{w}_h \in B_w(K). \end{array}\right. \tag{4.1}$$

Choosing $\widetilde{v}_h$ and $\widetilde{w}_h$ arbitrarily in $H_0^1(K) \subset (H^1(K) \setminus \mathbb{R})$, we have that boundary terms in (4.1) disappear. Furthermore, using the continuous and dense injection of $H_0^1(K)$ in $L^2(K)$, yields the *strong form* of problem (2.1,2.2) in the interior of each element $K \in \mathcal{T}_h$

$$\left\{\begin{array}{ll} -\widetilde{\sigma}_{h,x} + (a\widetilde{u}_h)_{,x} & = r_h, \\ \kappa^{-1}\widetilde{\sigma}_h - \widetilde{u}_{h,x} & = s_h. \end{array}\right. \tag{4.2}$$

Taking now $\widetilde{v}_h$ and $\widetilde{w}_h$ arbitrarily in $H^1(K) \setminus \mathbb{R}$ and using (4.2), we get

$$(\sigma_h^A - au_h^A)\widetilde{v}_h|_{\partial K} = (\mu_h^A - a\lambda_h^A)\widetilde{v}_h|_{\partial K}, \qquad u_h^A\widetilde{w}_h|_{\partial K} = \lambda_h^A\widetilde{w}_h|_{\partial K}. \tag{4.3}$$

The second relation in (4.3) yields $u_h^A = \lambda_h^A$ at the nodes (that is, the continuity of u_h^A), while the first relation in (4.3) yields, after back substitution, $\sigma_h^A = \mu_h^A$ at the nodes (that is, the continuity of σ_h^A). The nodal continuity of the *total* advective-diffusive flux $\sigma_h^A - au_h^A$ is then automatically recovered provided that a is nodally continuous.

REMARK 3. *Continuity of the total flux for any advective speed $a(x)$ could be obtained by resorting to an alternative* DPG *formulation which includes a priori the*

advective flux in the definition of the "flux" unknown, i.e.

$$\sigma = \kappa\, u_{,x} - F_{adv}(u).$$

In order to carry out the required analytical computations, we assume henceforth that the problem coefficients are given constants over each element $K \in \mathcal{T}_h$, denoted by κ^i, a^i and f^i, respectively, so that $r_h = r_h^i$ and $s_h = s_h^i$.

To uniquely determine the fine scales $\widetilde{u}_h$, $\widetilde{\sigma}_h$ in the class of equivalence $(L^2(K) \setminus \mathbb{R})^2$, we integrate equation (4.2) over $K^i = [x_i, x_{i+1}]$ together with the conditions (3.5) and the constraint

$$\int_K \widetilde{u}_h\, dx = \int_K \widetilde{\sigma}_h\, dx = 0. \tag{4.4}$$

More on the meaning of these constraints in the next section. We finally obtain

$$\widetilde{u}_h = \frac{\kappa^i}{a^i}\left((a^i)^{-1} r_h + s_h\right)\left(1 - \frac{a^i h^i}{\kappa^i}\frac{e^{a^i(x-x_i)/\kappa^i}}{e^{a^i h^i/\kappa^i} - 1}\right) + (a^i)^{-1}\left(x - x_i - \frac{h^i}{2}\right) r_h,$$

$$\widetilde{\sigma}_h = \kappa^i\left((a^i)^{-1} r_h + s_h\right)\left(1 - \frac{a^i h^i}{\kappa^i}\frac{e^{a^i(x-x_i)/\kappa^i}}{e^{a^i h^i/\kappa^i} - 1}\right).$$

Due to conditions (4.4), the only nonvanishing fine scale term in (3.11) for $\mathbb{DPG}_h^0$ is $\int_K \kappa^{-1}\widetilde{\sigma}_h \overline{w}_h\, dx$. This can be expressed as

$$\int_{K^i} (\kappa^i)^{-1}\widetilde{\sigma}_h \overline{w}_h\, dx = (\overline{w}_{i+1} - \overline{w}_i)(a^i(\kappa^i)^{-1}\overline{\sigma}^i - f^i)\,\tau_{\rm opt},$$

denoting the linear finite element test function on the i-th element as $\overline{w}_h|_K = (1 - s)\overline{w}_i + s\,\overline{w}_{i+1}$, with $s = (x - x_i)/h^i$, $0 \le s \le 1$, the coordinate in the reference element $\widehat{K} = [0, 1]$. The quantity $\tau_{\rm opt}$ is the well known intrinsic time or stability parameter that ensures a nodally exact solution for piecewise constant f (second order accurate in the general case, see e.g. [9]), i.e.

$$\tau_{\rm opt} = \frac{h^i}{2|a^i|}\,\widetilde{\xi}_{\rm opt}(\alpha^i), \tag{4.5}$$

$\alpha^i = |a^i| h^i / 2\kappa^i$ being the Peclet number associated with element K^i and

$$\widetilde{\xi}_{\rm opt}(t) = \begin{cases} \coth(t) - \dfrac{1}{t}, & t \in \mathbb{R}, \\ 0, & t = 0. \end{cases} \tag{4.6}$$

4.2. Approximate Subgrid Models. The exact elimination procedure described in the previous section is actually applicable due to the simplifying hypotheses on the linear differential operator and on the form of the problem data. In the case of a different operator, e.g. a non-linear one, such a procedure is, in general, no longer feasible. Under such circumstances, we must resort to an approximate method, which we describe again in the case of the linear advection-diffusion problem, but that is applicable in principle to any kind of operator (see section 5 for an application to the Burgers equation).

We now solve (3.12) under conditions (3.5) in an approximate manner. To this end, we set throughout the section

$$U_h(K) = \Sigma_h(K) = \mathbb{P}_0(K), \qquad V_h(K) = W_h(K) = \mathbb{P}_1(K) \qquad \forall K \in \mathcal{T}_h,$$

which amounts to assuming the coarse trial and test scales to be modeled by the lowest order method of the DPG family. We also assume to dispose of suitable (yet unspecified) *finite dimensional* subspaces $B_{u,h}(K)$, $B_{\sigma,h}(K)$ (for the trial functions) and $B_{v,h}(K)$, $B_{w,h}(K)$ (for the test functions) of the *infinite dimensional* bubble spaces introduced in (3.2) and (3.7). Then we use once again a discontinuous Petrov-Galerkin method over each element to provide an approximate solution to (3.12), that yields

$$\left\{ \begin{array}{ll} \displaystyle\int_K (\widetilde{\sigma}_h - a\widetilde{u}_h)\widetilde{v}_{h,x}\,dx = \int_K r_h\widetilde{v}_h\,dx & \\ \qquad - \big((\overline{\sigma}_h - \overline{\mu}_h) - a(\overline{u}_h - \overline{\lambda}_h)\big)\,\widetilde{v}_h|_{\partial K} & \forall \widetilde{v}_h \in B_{v,h}(K), \\ \displaystyle\int_K \kappa^{-1}\widetilde{\sigma}_h\widetilde{w}_h\,dx + \int_K \widetilde{u}_h\widetilde{w}_{h,x}\,dx = \int_K s_h\widetilde{w}_h\,dx & \\ \qquad + (\overline{\lambda}_h - \overline{u}_h)\widetilde{w}_h|_{\partial K} & \forall \widetilde{w}_h \in B_{w,h}(K). \end{array} \right. \tag{4.7}$$

Though in principle several choices of the bubble spaces are possible, we describe in the following one such procedure, which has the advantage of showing a link between the multiscale variational method and the classical p enrichment approach, performed using hierarchical bases (see also section 4.3). Thus, in view of a hierarchical construction of the augmented spaces for both trial and test functions, we select

$$\begin{array}{ll} B_{u,h}(K) = \mathbb{P}_{k+1}(K), & B_{\sigma,h}(K) = \mathbb{P}_{k+1}(K), \\ B_{v,h}(K) = \mathbb{P}_{k+2}(K), & B_{w,h}(K) = \mathbb{P}_{k+2}(K), \end{array} \tag{4.8}$$

supplied with the following *orthogonality conditions* that are convenient for practical implementation of the method

$$\left\{ \begin{array}{ll} \displaystyle\int_K \overline{u}_h\widetilde{u}_h\,dx = 0 & \forall(\overline{u}_h, \widetilde{u}_h) \in (U_h(K) \times B_{u,h}(K)), \\ \displaystyle\int_K \overline{\sigma}_h\widetilde{\sigma}_h\,dx = 0 & \forall(\overline{\sigma}_h, \widetilde{\sigma}_h) \in (\Sigma_h(K) \times B_{\sigma,h}(K)), \end{array} \right. \tag{4.9}$$

and

$$\left\{ \begin{array}{ll} \displaystyle\int_K \overline{v}_h\widetilde{v}_h\,dx = 0 & \forall(\overline{v}_h, \widetilde{v}_h) \in (V_h(K) \times B_{v,h}(K)), \\ \displaystyle\int_K \overline{w}_h\widetilde{w}_h\,dx = 0 & \forall(\overline{w}_h, \widetilde{w}_h) \in (W_h(K) \times B_{w,h}(K)). \end{array} \right. \tag{4.10}$$

We can prove the following proposition which formalizes the aforementioned link between the multiscale approach and the hierarchical p enrichment method.

PROPOSITION 4.1. *Under the choice of spaces $U_h(K) = \Sigma_h(K) = \mathbb{P}_0(K)$, $V_h(K) = W_h(K) = \mathbb{P}_1(K)$, which characterizes the $\mathbb{DPG}_h^0$ method, plus the bubble spaces* (4.8) *and the conditions* (4.9,4.10)*, the multiscale DPG method with approximate subgrid model is equivalent to the plain $\mathbb{DPG}_h^{k+1}$ method, $k \geq 0$.*

Proof. Since the interface degrees of freedom of the DPG method are not affected by the multiscale procedure, it suffices to consider the internal variables. Then the

proof follows by recognizing that conditions (4.9,4.10) select, for any element K, each bubble space as a polynomial space of dimension equal to $k+1$. In particular, the maximal degree of the polynomials in the two pairs of bubble spaces is $k+1$ and $k+2$ for $B_{u,h}$, $B_{\sigma,h}$ and $B_{v,h}$, $B_{w,h}$, respectively. Moreover, these bubble polynomials are proportional to the Legendre polynomials of degree ranging from 1 to $k+1$ and from 2 to $k+2$ for the trial and test bubble spaces, respectively. Finally, the (internal) augmented solution (u_h^A, σ_h^A) and test functions (v_h^A, w_h^A) are sought in $(\mathbb{P}_{k+1})^2$ and $(\mathbb{P}_{k+2})^2$, respectively. □

REMARK 4. *Throughout the article we refer to the* DPG *multiscale formulation with approximate subgrid modeling as the* multiscale $\mathbb{DPG}_h^{0,k+1}$ *method,* $k \geq 0$*, where the first superscript refers to the polynomial degree of the trial coarse scale modeling and the second superscript refers to the polynomial degree of the enriching trial bubble space.*

REMARK 5. *It was shown in ref. [2] that, once the* plain DPG *method is equipped with a quadrature rule, the resulting discrete scheme is equivalent to an implicit Runge-Kutta method of the collocation type. In particular, the use of Gauss-Legendre quadratures yields the Kuntzmann-Butcher (Gauss) Runge-Kutta family of schemes, which exhibits maximal order for a given number of stages when applied to arbitrary differential operators. According to this view, the plain* $\mathbb{DPG}_h^k$ *method requires using the* $k+1$*-point Gauss-Legendre quadrature to attain maximal accuracy. Thus, when dealing with the multiscale* $\mathbb{DPG}_h^{0,k+1}$ *method, the use of* $k+2$ *Gauss-Legendre quadrature nodes is advisable, if not mandatory, to deal with the case of varying problem data* κ, a *and* f*.*

Having characterized the choice for the bubble trial and test function spaces, we provide an example of the fine scale elimination procedure in the case of the lowest order DPG element, i.e. $k=0$.

Using the orthogonality condition (4.9) for the trial spaces, since the coarse scales are modelled as constants on element interiors, the fine trial modes are null-averaged linear functions, $\widetilde{u}_h|_{K^i} = (1-2s)\,\widetilde{u}^i$, $\widetilde{u}^i$ being the fine scale degree of freedom on the i-th element. Considering now the orthogonality condition (4.10) for the test spaces, given that the coarse scales are linear, the fine modes are now the quadratic functions $\widetilde{v}_h|_{K^i} = (6s^2-6s+1)\,\widetilde{v}^i$, where $\widetilde{v}^i$ is the fine scale test degree of freedom on the i-th element. Notice that the (reference) fine scale test function $\widetilde{v}_h$ has zero average over $[0,1]$ and vanishes at the two Gauss-Legendre points $1/2 \pm \sqrt{3}/6$. Inserting now the discrete approximations to $\widetilde{u}_h$, $\widetilde{\sigma}_h$, $\widetilde{v}_h$, $\widetilde{w}_h$ into (4.7) and solving for the coefficients $\widetilde{u}^i$, $\widetilde{\sigma}^i$, we get

$$\begin{aligned} \widetilde{u}^i &= \frac{1}{2}\,(\overline{\lambda}_{i+1} - \overline{\lambda}_i), \\ \widetilde{\sigma}^i &= \frac{1}{2}\,(\overline{\mu}_{i+1} - \overline{\mu}_i). \end{aligned} \tag{4.11}$$

Once again, the only non-vanishing fine scale term in (3.11) is

$$\int_K \kappa^{-1} \widetilde{\sigma}_h \overline{w}_h \, dx = (\overline{w}_{i+1} - \overline{w}_i)\,\frac{h^i}{6\kappa^i}\,\widetilde{\sigma}^i. \tag{4.12}$$

Using once again (3.11), the discrete constitutive equations in the coarse scales write

$$\overline{\sigma}^i = \frac{\kappa^i}{h^i}\,(\overline{\lambda}_{i+1} - \overline{\lambda}_i), \tag{4.13}$$

while the discrete flux equations give

$$\overline{\mu}_i - \overline{\mu}_{i+1} - a^i(\overline{\lambda}_i - \overline{\lambda}_{i+1}) = f^i h^i. \tag{4.14}$$

Therefore, using $(4.11)_2$, (4.14) and (4.13), (4.12) yields

$$\int_K \kappa^{-1}\widetilde{\sigma}_h \overline{w}_h \, dx = (\overline{w}_{i+1} - \overline{w}_i)(a^i(\kappa^i)^{-1}\overline{\sigma}^i - f^i)\,\tau_B,$$

where τ_B is now an approximation to the exact solution $\tau_{\rm opt}$, and reads

$$\tau_B = \frac{h^i}{2|a^i|}\,\widetilde{\xi}_B(\alpha^i), \tag{4.15}$$

with

$$\widetilde{\xi}_B(t) = \frac{t}{3}, \qquad t \in \mathbb{R}. \tag{4.16}$$

It is interesting to observe that, since in a neighborhood of the origin

$$\widetilde{\xi}_{\rm opt}(t) = \frac{1}{t} + \frac{t}{3} - \frac{t^3}{45} + \ldots - \frac{1}{t},$$

we have

$$\widetilde{\xi}_{\rm B}(\alpha^i) = \widetilde{\xi}_{\rm opt}(\alpha^i) + \mathcal{O}(h^3),$$

which ensures fourth order accuracy to the scheme when f is piecewise constant. This could also be improved, by considering higher order discretizations for the local fine scale problem (4.7). The increase in accuracy of the approximate subgrid model will be demonstrated on several numerical examples in the next sections.

4.3. The Multiscale DPG Method as a Hierarchical Finite Element Formulation. In this section, we wish to briefly comment about the relationship between the DPG finite element method with variational multiscale modeling and the classical p enrichment approach, performed using hierarchical bases. A similar discussion with reference to the more classical Galerkin method is the topic of ref. [4].

The fact that the finite element bases are of a hierarchical nature is crucial, since it allows us to identify some of the degrees of freedom as associated with the faster modes while the others represent the slower resolvable ones. In fact, this identification would not be possible using, for example, standard Lagrangian bases. However, it is also important to realize that the elimination of the fine modes in favor of the coarse ones, equations (3.11) and (3.12), while fundamental for showing the effect of the former scales on the latter ones in the linear case, is irrelevant as far as the computed solution is concerned.

In other words, once the finite element spaces are chosen according to the criteria discussed in sections 3.1 and 4.2, if we were to solve the linear problem associated with the DPG multiscale formulation *directly* or through the two (successively) coupled subproblems (3.11) and (3.12), we would clearly get exactly the same result. This is rather evident, if one only considers that the process of eliminating the fine scales as functions of the coarse scales is nothing else than the *static condensation procedure* of the internal degrees of freedom in a hierarchical p method.

To summarize, for the linear case one could in principle proceed in two alternative but totally equivalent ways. In the first case, the faster modes are computed through equation (3.12) (or (4.7)) and then inserted into (3.11) to yield the sole coarse degrees of freedom. Alternatively, one could simply solve a larger linear system whose unknowns are *both* the fast and slow degrees of freedom, which are therefore computed *simultaneously*. Of course, in this latter case one must not forget that the faster degrees of freedom represent the fine unresolved modes, that therefore must be discarded. The solution must consequently be regarded as that obtained by the sole use of the coarse degrees of freedom. In particular, in the case of the plain $\mathbb{DPG}_h^{k+1}$, or equivalently, due to Proposition 4.1, of the multiscale $\mathbb{DPG}_h^{0,k+1}$ method with the special bubble spaces discussed therein, the faster degrees of freedom are associated with the bubble functions of degree up to $k+1$ and $k+2$ for the trial and test spaces, respectively, while the coarse degrees of freedom are the ones connected with the $\mathbb{DPG}_h^0$ part of the trial and test basis functions. Results and comments about the application of the DPG-multiscale formulation to the non-linear steady Burgers equation will be shown in section 5.

4.4. The Stabilizing Effect of Multiscale Modeling. The effects of the multiscale modeling go well beyond the increase in accuracy discussed above, and result into a stabilized finite element discretization of the advection-diffusion model problem. To show this, consider the solution to the advection-diffusion problem using the plain version of $\mathbb{DPG}_h^0$, i.e. with no multiscale modeling. For simplicity, we consider a uniform grid of size h and again we assume that a and κ are constant throughout the domain, while the source term f is piecewise constant. For each element $K^i \in \mathcal{T}_h$, $i = 0, \ldots, n-1$, we have the following linear system of algebraic equations

$$\left\{\begin{array}{lcl} \sigma^i \dfrac{h}{2\kappa} - u^i + \lambda_i & = & 0, \\ \sigma^i \dfrac{h}{2\kappa} + u^i - \lambda_{i+1} & = & 0, \\ -\sigma^i + a u^i - a\lambda_i + \mu_i & = & f^i \dfrac{h}{2}, \\ \sigma^i - a u^i + a\lambda_{i+1} - \mu_{i+1} & = & f^i \dfrac{h}{2}, \end{array}\right. \tag{4.17}$$

where σ^i, u^i are the degrees of freedom associated with the internal variables, λ_j and μ_j ($j = i, i+1$) are the degrees of freedom associated with the interface variables at nodes x_i and x_{i+1}, while f^i denotes the value of f in element K^i. System (4.17) can be written in matrix form as

$$\left\{\begin{array}{lcl} \boldsymbol{A}\boldsymbol{y} + \boldsymbol{B}\boldsymbol{\lambda} & = & \boldsymbol{0}, \\ \boldsymbol{C}\boldsymbol{y} + \boldsymbol{D}\boldsymbol{\lambda} + \boldsymbol{E}\boldsymbol{\mu} & = & \boldsymbol{f}, \end{array}\right. \tag{4.18}$$

where $\boldsymbol{y} = (\sigma^i, u^i)^T$, $\boldsymbol{\lambda} = (\lambda_i, \lambda_{i+1})^T$, $\boldsymbol{\mu} = (\mu_i, \mu_{i+1})^T$ and $\boldsymbol{f} = f^i h/2(1,1)^T$, and where the following matrices have been defined

$$\boldsymbol{A} = \begin{pmatrix} \dfrac{h}{2\kappa} & -1 \\ \dfrac{h}{2\kappa} & 1 \end{pmatrix}, \boldsymbol{B} = \begin{pmatrix} 1 & 0 \\ 0 & -1 \end{pmatrix}, \boldsymbol{C} = \begin{pmatrix} -1 & a \\ 1 & -a \end{pmatrix},$$

$$\boldsymbol{D} = \begin{pmatrix} -a & 0 \\ 0 & a \end{pmatrix}, \boldsymbol{E} = \boldsymbol{B},$$

with $\boldsymbol{A}, \boldsymbol{B}, \boldsymbol{C}, \boldsymbol{D}, \boldsymbol{E} \in \mathbb{R}^{2\times 2}$. Since $\boldsymbol{A}$ is an invertible matrix, we can eliminate the internal variables $\boldsymbol{y}$ in favor of the displacement interface variables $\boldsymbol{\lambda}$ to get

$$\boldsymbol{y} = -\boldsymbol{A}^{-1}\boldsymbol{B}\boldsymbol{\lambda}. \tag{4.19}$$

Then, since also $\boldsymbol{E}$ is invertible, we can do the same for the flux interface variables $\boldsymbol{\mu}$, to obtain

$$\boldsymbol{\mu} = \boldsymbol{E}^{-1}\left(\boldsymbol{f} - (\boldsymbol{D} - \boldsymbol{C}\boldsymbol{A}^{-1}\boldsymbol{B})\boldsymbol{\lambda}\right). \tag{4.20}$$

Relations (4.19) and (4.20) hold for each element $K^i \in \mathcal{T}_h$, $i = 0, \ldots, n-1$. In particular, it is seen that, once the nodal displacement variables $\boldsymbol{\lambda}$ are computed, one can easily recover both the flux interface variables and the internal variables, whenever needed, by simple element-by-element post-processing.

Imposing now the continuity of the interface variable μ_h at each *internal* node x_i, $i = 1, \ldots, n-1$, we eventually end up with the following square linear algebraic system of size $n-1$ in the nodal unknowns λ_j

$$-(1+\gamma)\lambda_{i-1} + 2\lambda_i - (1-\gamma)\lambda_{i+1} = (f^i + f^{i+1})\frac{h^2}{2\kappa}, \qquad i = 1, \ldots, n-1, \tag{4.21}$$

where $\lambda_0 = g(0)$, $\lambda_n = g(X)$ and $\gamma = ah/2\kappa$. It is immediate to check that for $\alpha = |\gamma| \leq 1$, the matrix associated with (4.21) is an M-matrix, since its off-diagonal terms are non-positive and its principal minors are all positive. This property provides stability to the discrete formulation and ensures that a discrete maximum principle holds for the plain version of $\mathbb{DPG}_h^0$ (see [12]). The M-matrix property is clearly lost for $\alpha > 1$, and the solution will be highly oscillatory in this case.

Using now $\mathbb{DPG}_h^0$ with the approximate subgrid model and following the same static condensation procedure as before, we get

$$\begin{aligned} &-\big(1+\gamma\big(1+\widetilde{\xi}_{\mathrm{B}}(\gamma)\big)\big)\overline{\lambda}_{i-1} + 2\left(1+\gamma\widetilde{\xi}_{\mathrm{B}}(\gamma)\right)\overline{\lambda}_i - \big(1-\gamma\big(1-\widetilde{\xi}_{\mathrm{B}}(\gamma)\big)\big)\overline{\lambda}_{i+1} \\ &\qquad = \big((1+\widetilde{\xi}_{\mathrm{B}}(\gamma))f^i + (1-\widetilde{\xi}_{\mathrm{B}}(\gamma))f^{i+1}\big)\frac{h^2}{2\kappa}, \qquad i = 1, \ldots, n-1, \end{aligned} \tag{4.22}$$

which gives an M-matrix for any α. Hence the solution will not oscillate even for arbitrarily large values of the local Peclet number. The approximate subgrid result should be compared with the one obtained with the exact subgrid model, that gives

$$\begin{aligned} &-\big(1+\gamma\big(1+\widetilde{\xi}_{\mathrm{opt}}(\gamma)\big)\big)\overline{\lambda}_{i-1} + 2\left(1+\gamma\widetilde{\xi}_{\mathrm{opt}}(\gamma)\right)\overline{\lambda}_i - \big(1-\gamma\big(1-\widetilde{\xi}_{\mathrm{opt}}(\gamma)\big)\big)\overline{\lambda}_{i+1} \\ &\qquad = \big((1+\widetilde{\xi}_{\mathrm{opt}}(\gamma))f^i + (1-\widetilde{\xi}_{\mathrm{opt}}(\gamma))f^{i+1}\big)\frac{h^2}{2\kappa}, \qquad i = 1, \ldots, n-1. \end{aligned} \tag{4.23}$$

4.5. Numerical Validation for the Linear Case. We now test the proposed formulation on a practical example. In order to measure the convergence rate of the method, we need to introduce appropriate norms. At first, we denote by $I_{1,K}(v)$ the approximation of $\int_K v\,dx$ using the trapezoidal rule for any function $v \in L^2(\Omega)$ that is also sufficiently smooth on each $K \in \mathcal{T}_h$. Moreover, for each $K \in \mathcal{T}_h$ we denote by $\{\overline{x}_{j,K}^k\}_{j=0}^k$ the $k+1$ Gauss-Legendre points on K, $k \geq 0$. At this point we can define

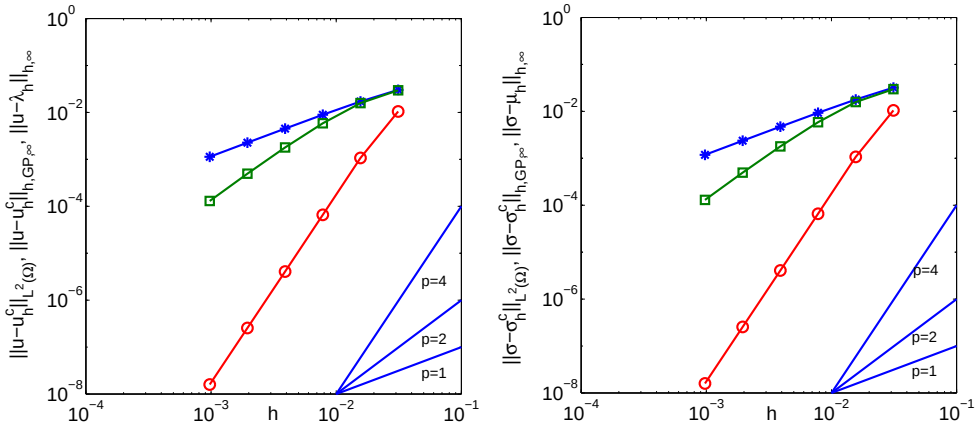

FIG. 4.1. *Error curves for the coarse scales in the linear case: errors in u (left) and σ (right) for the approximate subgrid multiscale model using $\mathbb{DPG}_h^0$ finite elements.*

the following three norms:

$$\|v\|_{h,L^2(\Omega)} = \left(\sum_{i=0}^{n-1} I_{1,K^i}(v^2) \right)^{1/2},$$
$$\|w\|_{h,GP,\infty} = \max_{0 \le i \le n-1} \left(\max_{0 \le j \le k} |w(\overline{x}^k_{j,K^i})| \right),$$
$$\|\eta\|_{h,\infty} = \max_{0 \le i \le n} |\eta_i|,$$

where w is any bounded function defined at the Gauss points of $\mathcal{T}_h$ and η is any bounded function defined at the nodes of $\mathcal{T}_h$. The first one is a discrete $L^2(\Omega)$ norm, while the other two norms are discrete maximum norms over the set of Gauss points and $\mathcal{E}_h$, respectively. The quadrature formula used in the discrete norm is accurate enough not to pollute the computed accuracy, and at the same time avoids to sample the solution at superconvergent points. The cases $k = 0$ and $k = 1$ have been considered in the numerical experiments reported below.

The following symbols are used in the graphs: for any h, symbol '*' refers to $\|\cdot\|_{h,L^2(\Omega)}$, while symbols '□' and 'o' denote $\|\cdot\|_{h,GP,\infty}$ and $\|\cdot\|_{h,\infty}$, respectively. Finally, in all figure labels the symbol $(\cdot)^c = \overline{(\cdot)}$ indicates the coarse scales.

The convergence behavior of the approximate subgrid model for $\mathbb{DPG}_h^0$ is compared on the solution of problem (2.1) with $X = 1$, $u(0) = u(X) = 0$, $a = 1$, $\kappa = 1 \cdot 10^{-2}$ and $f = x^2$. We show in figure 4.1 the errors between the analytical solution and the computed coarse scales in the appropriate norms as functions of h. Fourth order convergence is observed for the interface fields, while the internal field errors measured in the L^2 norm are only first order accurate. The accuracy of these fields increases when the errors are measured in the discrete Gauss point maximum norm.

The fourth order accuracy of the boundary unknowns can be explained by recalling that the multiscale $\mathbb{DPG}_h^0$ with approximate subgrid modeling coincides with the plain $\mathbb{DPG}_h^1$ using a hierarchical base (see Proposition 4.1 and the concluding remark of section 4.2). Since the order of $\mathbb{DPG}_h^k$ for any non-linear problem is $2(k+1)$ for the interface unknowns [2], we should indeed observe fourth order accuracy for these

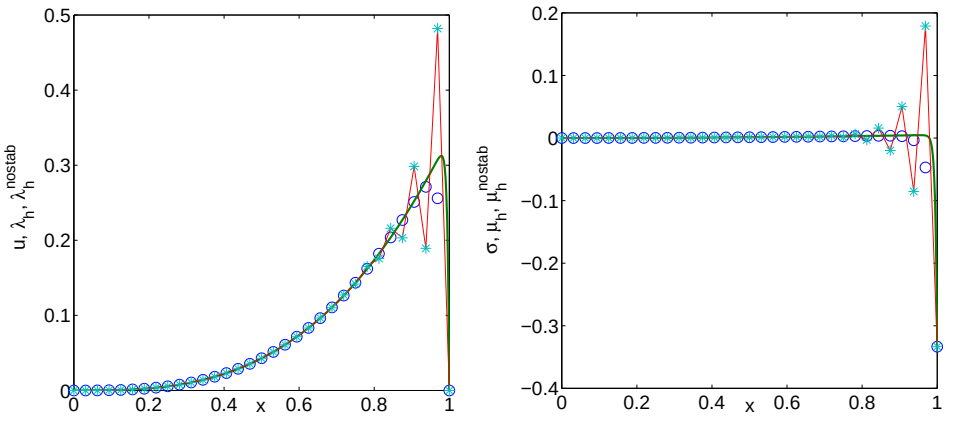

FIG. 4.2. *Solution in terms of the nodal values λ_h and μ_h using $\mathbb{DPG}_h^0$ finite elements for the linear problem. Solid line: analytical solution; $*$: no multiscale stabilization; $\circ$: approximate subgrid model.*

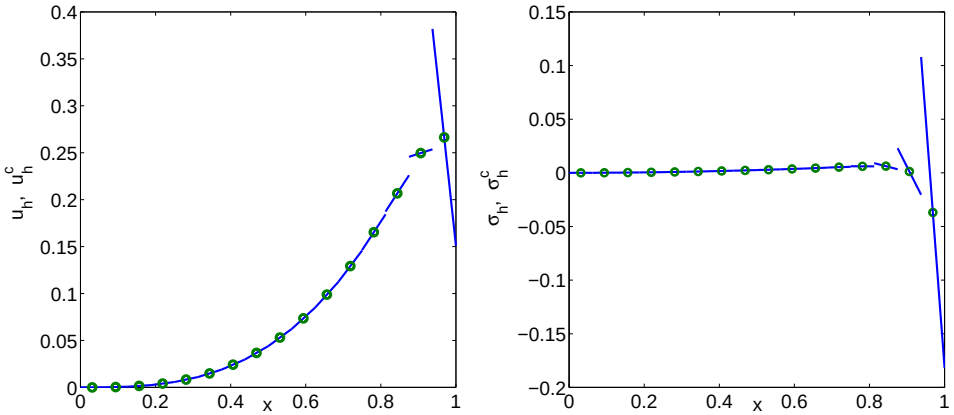

FIG. 4.3. *Solution in terms of the internal values $\overline{u}_h$, $\widetilde{u}_h$ and $\overline{\sigma}_h$, $\widetilde{\sigma}_h$ using multiscale $\mathbb{DPG}_h^0$ finite elements for the linear problem. $\circ$: coarse scale centered at the mid point of each element; solid line: fine modes.*

fields. The internal unknowns are then only first order accurate in the L^2 norm because we are discarding from the solution its linear components $\widetilde{u}_h$, $\widetilde{\sigma}_h$, since they are here interpreted as the unresolved modes. By retaining the linear components, we would indeed achieve a higher accuracy for the internal unknowns at the price, however, to loose the stabilizing properties of the multiscale formulation. This last statement will be verified in the next section, in the case of the non-linear steady Burgers equation. Similar results are discussed at greater length in the context of the Galerkin method in ref. [4]. The solutions in terms of the nodal values λ_h and μ_h are shown in figure 4.2 for the case $\kappa = 5 \cdot 10^{-3}$ and $h = 1/32$ for the plain $\mathbb{DPG}_h^0$ finite element formulation and $\mathbb{DPG}_h^0$ equipped with the approximate subgrid model. Although both schemes are asymptotically second order accurate, the oscillating nature of the solution computed by $\mathbb{DPG}_h^0$ should be contrasted with the smooth behavior of the stabilized scheme. Finally, figure 4.3 shows the solutions in terms of the internal values $\overline{u}_h$, $\widetilde{u}_h$ and $\overline{\sigma}_h$, $\widetilde{\sigma}_h$ for the case $\kappa = 1 \cdot 10^{-2}$ and $h = 1/16$ using the approximate

subgrid model. The coarse scales $\overline{u}_h$ and $\overline{\sigma}_h$ are represented as circles centered at the mid point of each element since they are constant at the element level, while the fine scale solutions are linear function with null mean value, as previously explained.

5. The Non-linear Advection-Diffusion Problem. We consider now the classical steady Burgers equation, where the convective flux reads

$$F_{\text{adv}}(u) = \frac{1}{2}\,u^2.$$

The plain DPG method applied to this model problem yields

$$\left\{\begin{array}{ll} \displaystyle\int_K (\sigma_h - \frac{1}{2}\,u_h^2) v_{h,x}\,dx - (\mu_h - \frac{1}{2}\,\lambda_h^2) v_h|_{\partial K} = \int_K f v_h\,dx & \forall v_h \in V_h(K), \\ \displaystyle\int_K \kappa^{-1}\sigma_h w_h\,dx + \int_K u_h w_{h,x}\,dx - \lambda_h w_h|_{\partial K} = 0 & \forall w_h \in W_h(K). \end{array}\right. \tag{5.1}$$

Once again we consider the multiscale $\mathbb{DPG}_h^{0,0}$ for simplicity. The choice of the trial and test functions is identical to the previously discussed linear case, and in particular

$$\left\{\begin{array}{l} u_h|_{K^i} = \overline{u}^i + (1-2s)\,\widetilde{u}^i \in \mathbb{P}_0(K^i) \oplus B_{u,h}(K^i), \\ v_h|_{K^i} = (1-s)\,\overline{v}_i + s\,\overline{v}_{i+1} + (6s^2 - 6s + 1)\,\widetilde{v}^i \in \mathbb{P}_1(K^i) \oplus B_{v,h}(K^i), \end{array}\right. \tag{5.2}$$

where $s = (x - x_i)/h^i$, and similarly for $\sigma_h|_{K^i}$ and $w_h|_{K^i}$. The resulting discrete non-linear problem can then be solved by Newton's method as anticipated in section 3.2.

At this point it is clear that the solution of a non-linear problem can proceed along the same identical guidelines as a linear(ized) problem (see section 4.2), and does not differ from the solution of any non-linear finite element problem when a hierarchical basis is used. In fact, we can either eliminate the fine scale corrections at each Newton iterate in favor of the coarse scale corrections, or we can solve a larger problem where both corrections are computed simultaneously. Either way, the final (converged) solution will be identical, and we just need to consider the coarse scale degrees of freedom. For simplicity of implementation, the second approach was chosen in this work, to the possible price of a slightly larger computational cost (of no great significance in this one-dimensional setting).

Some remarks are in order about the non-linear case. First of all, it should be noted that the analogy with stabilized methods, i.e. methods that make use of stability parameters of the sort of the previously encountered τ_{opt} and τ_B, does not hold any more in this case, since the elimination of the fine scales in favor of the coarse residuals is, in general, no longer possible. Second, the use of Newton method for approximating the solution to a non-linear problem, yields a linearized problem for the *corrections* of the interface unknown λ_h whose stiffness matrix is an M-matrix, analogously to the linear case of section 4.4. Since the non-linear solution is obtained by adding a finite number of corrections, and each correction is monotone, even the non-linear solution will be monotone. Therefore, even in the non-linear case the multiscale solution can not oscillate. This observation has been anticipated in ref. [4] for the multiscale version of the Galerkin method.

5.1. Numerical Validation for the Non-linear Case. The solution to the non-linear problem (5.1) was computed with the proposed method for the case $\kappa = 1 \cdot 10^{-2}$, $X = 1$, $u(0) = 1$, $u(X) = 0$ and $f = 0$. Figure 5.1 plots the errors in the

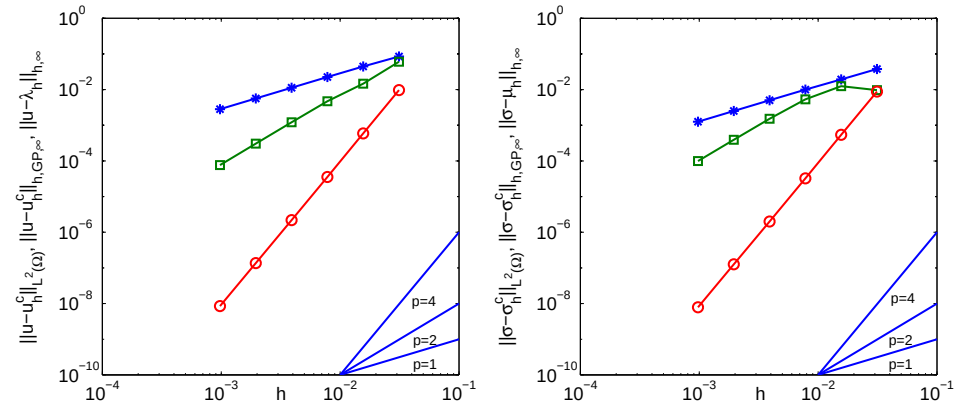

FIG. 5.1. *Error curves for the coarse scales in the non-linear case: errors in u (left) and σ (right) for the approximate subgrid multiscale model using $\mathbb{DPG}_h^0$ finite elements.*

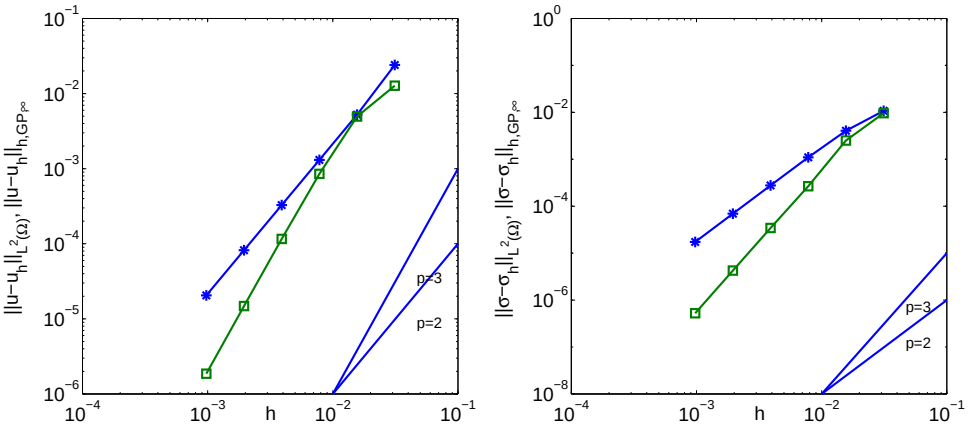

FIG. 5.2. *Error curves for the complete solution (coarse + fine) in the non-linear case: errors in u (left) and σ (right) for the approximate subgrid multiscale model using $\mathbb{DPG}_h^0$ finite elements.*

various computed fields using the appropriate norms, in terms of the discretization parameter h. The same convergence behavior observed in the linear case is here confirmed even for the non-linear problem. In particular, fourth order convergence is observed for all computed interface variables, while linear convergence is obtained for the internal variables when measured in the L^2 norm, see figure 5.1.

By retaining the linear components, a higher accuracy is achieved for the internal unknowns, as shown in figure 5.2, however, the stabilizing properties of the multiscale formulation are lost, as anticipated in the previous section. Second order convergence can be obtained also for the internal fields when sampling them at the (two) Gauss-Legendre points (see remark 5).

Figure 5.3 plots the computed solutions in terms of the interface fields λ_h and μ_h obtained in the case $h = 1/32$ and compares them with the analytical ones. The stabilizing effects of the proposed method are evident even in this non-linear case. Finally, figure 5.4 shows the solutions in terms of the internal values $\overline{u}_h$, $\widetilde{u}_h$ and $\overline{\sigma}_h$, $\widetilde{\sigma}_h$ for the case $h = 1/16$.

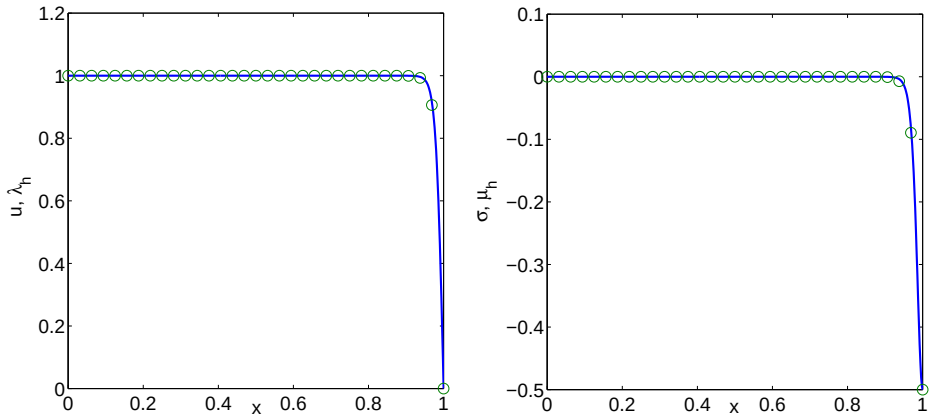

FIG. 5.3. *Solution in terms of the nodal values λ_h and μ_h using $\mathbb{DPG}_h^0$ finite elements for the non-linear steady Burgers equation. Solid line: analytical solution; ∘: approximate subgrid model.*

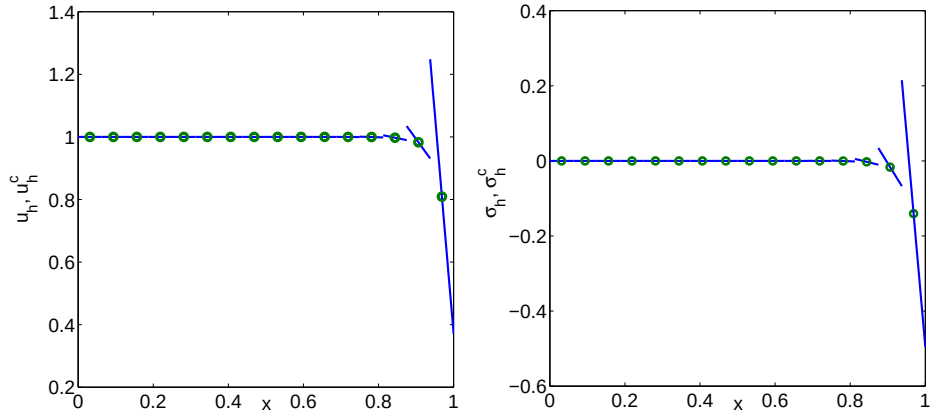

FIG. 5.4. *Solution in terms of the internal values $\overline{u}_h$, $\widetilde{u}_h$ and $\overline{\sigma}_h$, $\widetilde{\sigma}_h$ using multiscale $\mathbb{DPG}_h^0$ finite elements for the non-linear steady Burgers equation. ∘: coarse scale centered at the mid point of each element; solid line: fine modes.*

6. Conclusions. We have analyzed the application of the variational multiscale method to the DPG formulation of the one-dimensional advection-diffusion model problem with both linear and non-linear constitutive relations for the advective flux. Using the the multiscale framework, we have shown the equivalence between the plain $\mathbb{DPG}_h^{k+1}$ and the multiscale $\mathbb{DPG}_h^{0,k+1}$ methods for a particular choice of the approximate subgrid scales. We have enforced general orthogonality conditions for the fine and coarse splittings of the test and trial spaces, which can be used for conveniently constructing hierarchical multiscale p methods. We remark that these orthogonality conditions are not necessary but turn out to be practical for implementation. Moreover, the above ideas can be extended to multi-dimensional problems.

We have analyzed both the exact and the approximate elimination of the fine modes for the linear problem. In the former case, we recover the well known optimal stabilization parameter that ensures a nodally exact scheme, as expected. In the latter case, we obtain a consistent approximation of the optimal stabilization parameter, that increases the order of the basic underlying finite element method and avoids the

appearance of spurious oscillations in the numerical solution. We have numerically investigated the scheme when applied to a non-linear model problem, reaching similar conclusions as in the linear case.

7. Acknowledgment. This research was supported by the M.U.R.S.T. Cofin 2001 Grant "Metodi Numerici Avanzati per Equazioni Parziali di Interesse Applicativo", and by the Large Scale Computing (LSC) initiative at Politecnico di Milano through the research project "IPACS: Interdisciplinary Parallel Adaptive CFD Solvers".

REFERENCES

[1] D.N. Arnold, F. Brezzi, B. Cockburn and L.D. Marini, *Discontinuous Galerkin methods for elliptic problems*, in Discontinuous Galerkin Methods, Eds.: B. Cockburn, G.E. Karniadakis and C.W. Shu, Lecture Notes in Computational Science and Engineering, 11, Springer, 89–101 (2000).

[2] C.L. Bottasso, *A new look at finite elements in time: a variational interpretation of Runge-Kutta methods*, Appl. Numer. Math., 25, (1997), pp. 355–368.

[3] C.L. Bottasso, P. Causin, S. Micheletti and R. Sacco *A discontinuous Petrov-Galerkin method: application to the elasticity and advection-diffusion models*, SIMAI2002 Conference, Chia Laguna (CA), Italy, May 27-31, 2002.

[4] C.L. Bottasso and D. Detomi, *An investigation into the self-stabilizing properties of the p version of the Galerkin method in the one-dimensional case*, Comput. Methods Appl. Mech. Engrg., under review.

[5] C.L. Bottasso, S. Micheletti and R. Sacco, *The discontinuous Petrov-Galerkin method for elliptic problems*, Comput. Methods Appl. Mech. Engrg., 191 (2002), pp. 3391–3409.

[6] F. Brezzi, *Recent results in the treatment of subgrid scales*, ESAIM, 32ème Congrès d'Analyse Numérique CANUM2000, Vol. 8, September, 2000.

[7] P. Causin and R. Sacco, *A discontinuous Petrov–Galerkin method with lagrangian multipliers for second order elliptic problems*, MOX-report n. 19, May 2003, Modeling and Scientific Computing, Dipartimento di Matematica "F. Brioschi", Politecnico di Milano, Milano, Italy. SIAM J. Numer. Anal., under review.

[8] P. Causin and R. Sacco, *Mixed-hybrid Galerkin and Petrov-Galerkin finite element formulations in continuum mechanics*, in Proceedings of the Fifth World Congress on Computational Mechanics (WCCM V), Vienna, Austria, Eds.: H.A. Mang, F.G. Rammerstorfer, J. Eberhardsteiner, ISBN 3-9501554-0-6, http://wccm.tuwien.ac.at, July 7-12, 2002.

[9] E. Gatti, S. Micheletti and R. Sacco, *A new Galerkin framework for the drift-diffusion equation in semiconductors*, East West J. Numer. Math., 6, (1998), pp. 101–135.

[10] T.J.R. Hughes, G. Engel, L. Mazzei and M.G. Larson, *The continuous Galerkin method is locally conservative*, J. Comput. Phys., 163 (2000), pp. 467–488.

[11] T.J.R. Hughes, G.R. Feijóo, L. Mazzei and J.B. Quincy, *The variational multiscale method – a paradigm for computational mechanics*, Comput. Methods Appl. Mech. Engrg., 166 (1998), pp. 3–24.

[12] H.G. Roos, M. Stynes and L. Tobiska, *Numerical Methods for Singularly Perturbed Differential Equations*, Springer-Verlag, Berlin, Germany (1996).